

Study for (anti)hypertriton and light (anti)nuclei productions in high energy collisions at $\sqrt{S_{NN}} = 200$ GeV

Hai-Jun Li,^{1,*} Ting-Ting Zeng,¹ and Gang Chen¹

¹*School of Mathematics and Physics, China University of Geosciences, Wuhan 430074, China*

We use the parton and hadron cascade (PACIAE) model and the dynamically constrained phase-space coalescence (DCPC) model to investigate the productions of (anti)hypertriton and light (anti)nuclei generated by 0-10% centrality $^{12}\text{C}+^{12}\text{C}$, $^{24}\text{Mg}+^{24}\text{Mg}$, $^{40}\text{Ca}+^{40}\text{Ca}$, and $^{64}\text{Cu}+^{64}\text{Cu}$ collisions at $\sqrt{S_{NN}} = 200$ GeV with $|y| < 1.5$ and $p_T < 5$. We study the yield ratios of the antiparticle to particle and the rapidity distributions of the different (anti)nuclei. We find that the amounts of antimatter produced are significantly lower than that of the corresponding particles, the results of theoretical models are well consistent with the PHOBOS data. The yield ratios of the particle to antiparticle in different transverse momentum regions are also given, and we find that the ratios are raise with the increase of the transverse momentum.

I. INTRODUCTION

In 1928, Dirac predicted the existence of negative energy states (i.e., antimatter) of the electrons depending on the symmetry principle of the quantum mechanics for the first time [1]. According to the Big Bang theory [2], it is generally accepted that equal amounts of matter and antimatter have been produced during the initial state of the Universe. However, this symmetry got lost in a series of evolutions of the Universe with no significant amount of antimatter exist now [3]. Since the high energy ultrarelativistic heavy-ion collisions could create abundant hyperons and nucleons, and the initial fireballs produced by the heavy-ion collisions are very similar to the Universe initial state, so the study of antinuclei productions in heavy-ion collisions maybe a better choice to solve above puzzle [4]. However, since the low abundance of the light nuclei (antinuclei) and the antimatter are unstable, the research of their productions may be quite difficult both in theoretically and experimentally [5].

The antimatter nuclei have been widely studied in cosmic ray [6, 7] and accelerator experiments [8, 9], which could be the indirect signals of the new physics, such as the dark matter (DM) and the manmade matter called quark gluon plasma (QGP) [10, 11]. Hypernuclei provide a doorway to the productions of strangelets and a unique opportunity to study the hyperon-nucleon (YN) and hyperon-hyperon (YY) interactions [12]. The measurements of YN and YY interactions are essential for the theoretical study of neutron stars [13] and exotic states of finite nuclei [14]. In 2010, the STAR Collaboration reported their measurements of $^3_{\Lambda}\text{H}$ and $^3_{\bar{\Lambda}}\text{H}$ productions in Au+Au collisions at top Relativistic Heavy-Ion Collider (RHIC) energy [15], including 70 ± 17 antihypertritons ($^3_{\bar{\Lambda}}\text{H}$) and 157 ± 30 hypertritons ($^3_{\Lambda}\text{H}$) in the 8.9×10^7 minimum-bias and 2.2×10^7 central (head-on) Au+Au collision events. Additionally, they also reported 18 ^4He counts at RHIC in 10^9 recorded Au+Au collisions at the center-of-mass energies of 200 GeV and 62 GeV per nucleon-nucleon pair in 2011 [16]. Therefore, we have the simulation study about the productions of (anti)hypertriton and light (anti)nuclei at high energy (200 GeV) in $^{12}\text{C}+^{12}\text{C}$, $^{24}\text{Mg}+^{24}\text{Mg}$, $^{40}\text{Ca}+^{40}\text{Ca}$, and $^{64}\text{Cu}+^{64}\text{Cu}$ collisions.

We have proposed a dynamically constrained phase-space coalescence (DCPC) model [17] based on the parton and hadron cascade (PACIAE) model [18, 19]. We have predicted the light nuclei (antinuclei) yields, transverse momentum distributions, and the rapidity distributions in pp collisions at 7 and 14 TeV [17]. We also have investigated the light nuclei (antinuclei), hypernuclei (antihypernuclei) productions [5] and studied their centrality dependence [20], scaling feature [21] in the 0-5% most central Au+Au collisions at 200 GeV. Thus, these works make the study for the (anti)hypertriton and light (anti)nuclei productions in nucleon-nucleon (NN) collisions possible.

This paper is structured as follows. In Sec. II, the PACIAE model coupled with the DCPC model are developed to study the production rates of hypertriton ($^3_{\Lambda}\text{H}$) and light nuclei, i.e. d , t , and ^3He corresponding to their antimatter in high energy collisions. In Sec. III, we calculate the yield ratios of antiparticle to particle in $^{12}\text{C}+^{12}\text{C}$, $^{24}\text{Mg}+^{24}\text{Mg}$, $^{40}\text{Ca}+^{40}\text{Ca}$, and $^{64}\text{Cu}+^{64}\text{Cu}$ collisions with the beams of energy at $\sqrt{S_{NN}} = 200$ GeV. The studies of the rapidity distributions and the transverse momentum distributions of d/\bar{d} , t/\bar{t} , $^3\text{He}/^3\bar{\text{He}}$ and $^3_{\Lambda}\text{H}/^3_{\bar{\Lambda}}\text{H}$ are also given. The conclusion is given in Sec. IV.

*Electronic address: lhj718@foxmail.com

II. MODELS

In this section, we briefly introduce the PACIAE and DCPC models. The PYTHIA model (PYTHIA 6.4 [22]) is designed for the high energy hadron-hadron collisions. The process of hadron-hadron collisions can be described by the parton-parton collisions in PYTHIA. The QCD radiation initial/final states and the multi-parton interactions are also considered. The final hadron states can be eventually derived by the hadron-hadron collisions. The PACIAE [18, 19] model is based on PYTHIA 6.4, which is designed for the nucleus-nucleus collisions. In PACIAE, the nucleus-nucleus collisions can be described by the nucleon-nucleon (NN) collisions. The initial parton state, composed of quarks/antiquarks and gluons, is regarded as the quark-gluon matter (QGM) generated in the relativistic nucleus-nucleus collision. The rescattering among the QGM partons can be described by the $2 \rightarrow 2$ Lo-pQCD parton-parton cross sections [23]. In order to describe the high order and the nonperturbative corrections, the K factor is added in the model. The hadronic matter continues to scatter until hadronic freeze-out [24, 25]. More details about these models can be found in Ref. [19].

According to the uncertainty principle of the quantum statistical mechanics

$$\Delta\vec{q}\Delta\vec{p} \geq h^3, \quad (1)$$

we could not give the precisely informations of both the position $\vec{q} = (x, y, z)$ and the momentum $\vec{p} = (p_x, p_y, p_z)$ of a particle in the six-dimension phase space. The yield of a single particle can be described by

$$\int_{\mathcal{H} \leq \mathcal{E}} \frac{d\vec{q}d\vec{p}}{h^3}, \quad (2)$$

with the Hamiltonian \mathcal{H} and the energy \mathcal{E} of the particle. Thus, we can only derive the particle lies inside a quantum “box” or “state” in a six-dimension phase space with a phase space volume of $\Delta\vec{q}\Delta\vec{p}$. Additionally, we can derive the yield for the N -particle system

$$\int \dots \int_{\mathcal{H} \leq \mathcal{E}} \frac{d\vec{q}_1 d\vec{p}_1 \dots d\vec{q}_N d\vec{p}_N}{h^{3N}}. \quad (3)$$

In this work, in order to obtain the yield of $\overline{\overline{\overline{\frac{3}{\Lambda}\text{H}}}}$ in the DCPC model, we have

$$y = \int \dots \int \delta_{123} \frac{d\vec{q}_1 d\vec{p}_1 d\vec{q}_2 d\vec{p}_2 d\vec{q}_3 d\vec{p}_3}{h^9}, \quad (4)$$

$$\delta_{123} = \begin{cases} 1 & \text{if } 1 = \bar{p}, 2 = \bar{n}, 3 = \bar{\Lambda}, \text{ combination;} \\ & m_0 \leq m_{\text{inv}} \leq m_0 + \Delta m; \\ & |q_{ij}| \leq D_0, (i \neq j; i, j = 1, 2, 3); \\ 0 & \text{otherwise;} \end{cases} \quad (5)$$

with the rest mass of $\overline{\overline{\overline{\frac{3}{\Lambda}\text{H}}}}$, m_0 , the diameter D_0 , the allowed mass uncertainty Δm , and the vector distance between particles i and j , $|\vec{q}_{ij}| = |\vec{q}_i - \vec{q}_j|$, where

$$m_{\text{inv}} = \left[\left(\sum_{i=1}^3 \mathcal{E}_i \right)^2 - \left(\sum_{i=1}^3 \vec{p}_i \right)^2 \right]^{1/2}, \quad (6)$$

with the particle energy ($\mathcal{E}_1, \mathcal{E}_2, \mathcal{E}_3$) and momentum ($\vec{p}_1, \vec{p}_2, \vec{p}_3$). Then we can derive the configuration of the $\overline{\overline{\overline{\frac{3}{\Lambda}\text{H}}}}$ ($\bar{p} + \bar{n} + \bar{\Lambda}$) system from a single event

$$C_{\bar{p}\bar{n}\bar{\Lambda}}(\Delta q_i; \vec{p}_i), (i = 1, 2, 3), \quad (7)$$

The diameter constraint in Eq. (5) can be taken as

$$\Delta q_i \leq R_0, (i = 1, 2, 3), \quad (8)$$

with the radius of $\overline{\overline{\overline{\frac{3}{\Lambda}\text{H}}}}$, R_0 .

Above configurations contribute the partial yield to $\overline{\overline{\overline{\frac{3}{\Lambda}\text{H}}}}$ with

$$y_{123} = \begin{cases} 1 & \text{if } m_0 \leq m_{\text{inv}} \leq m_0 + \Delta m, \\ 0 & \text{otherwise;} \end{cases} \quad (9)$$

Therefore, we can derive the whole yield of $\overline{\overline{\overline{\frac{3}{\Lambda}\text{H}}}}$ from a single event by the sum of the partial yield configurations of Eq. (7) and the combinations.

TABLE I: The integrated yield dN/dy of particles with 0 – 10% centrality, for p , \bar{p} , Λ , and $\bar{\Lambda}$ in $^{64}\text{Cu}+^{64}\text{Cu}$ collisions at $\sqrt{S_{NN}} = 62.4$ GeV and $\sqrt{S_{NN}} = 200$ GeV.

Particle type	62.4(GeV)		200(GeV)	
	PACIAE	PHENIX ^a	PACIAE	STAR ^b
p	4.49	4.54	7.48	
\bar{p}	2.57	2.73	4.82	
Λ	2.18		4.75	4.68 ± 0.45
$\bar{\Lambda}$	1.45		3.58	3.79 ± 0.37

^a The PHENIX data are taken from Ref. [26].

^b The STAR data are taken from Ref. [27].

III. RESULTS AND DISCUSSION

We use the PACIAE [18, 19] model to generate the final state of the particles. The hyperons are heavier than Λ in the PACIAE model. The values of the model parameters are fixed with the values given by PYTHIA model. Additionally, the values of the parameters K factor, $\text{parj}(1)$, $\text{parj}(2)$, and $\text{parj}(3)$, corresponding to the PYTHIA strange productions, are given by fitting the PHENIX data of p , \bar{p} in Cu+Cu collisions at $\sqrt{S_{NN}} = 62.4$ GeV by the 0-10% centrality with $3.0 < |y| < 3.9$ and $0.5 < p_T < 4.5$ [26] and the STAR data of Λ , $\bar{\Lambda}$ in Cu+Cu collisions at $\sqrt{S_{NN}} = 200$ GeV by the 0 – 10% centrality with $|y| < 0.5$ and $p_T < 5$ [27], which are shown in Tab. I. Then we have the fitted parameters with $K = 3$, $\text{parj}(1) = 0.15$, $\text{parj}(2) = 0.45$, and $\text{parj}(3) = 0.65$. The yields dN/dy of \bar{d} is calculated by the DCPC model in Cu+Cu collisions at $\sqrt{S_{NN}} = 200$ GeV by 0 – 10% centrality with $|y| < 0.9$ and $0.2 < p_T < 0.9$, we calculate the $\Delta m = 0.0003$. The results from our model agree well with the experimental data from the STAR Collaboration [27].

We generate 5×10^7 minimum-bias events by the PACIAE model in $^{12}\text{C}+^{12}\text{C}$, $^{24}\text{Mg}+^{24}\text{Mg}$, $^{40}\text{Ca}+^{40}\text{Ca}$, and $^{64}\text{Cu}+^{64}\text{Cu}$ collisions at $\sqrt{S_{NN}} = 200$ GeV, the rapidity region we selected is $|y| < 1.5$, and the transverse momentum region is $0 < p_T < 5$ (GeV/c). The integrated yields dN/dy of (anti)hypertriton $^3_{\Lambda}\text{H}$ ($^3_{\Lambda}\bar{\text{H}}$) and light (anti)nuclei d (\bar{d}), t (\bar{t}), and ^3He ($^3\bar{\text{He}}$) are simulated by the DCPC model, which are shown in Tab. II.

The yield ratios of antiparticle to particle are given in FIG. 1, including π^-/π^+ , K^-/K^+ , \bar{p}/p , \bar{n}/n , $\bar{\Lambda}/\Lambda$, $\bar{\Xi}^-/\Xi^-$, and $\bar{\Omega}^-/\Omega^-$. For the different collision nucleon, $^{12}\text{C}+^{12}\text{C}$, $^{24}\text{Mg}+^{24}\text{Mg}$, $^{40}\text{Ca}+^{40}\text{Ca}$, and $^{64}\text{Cu}+^{64}\text{Cu}$, the ratios of antiparticle to particle are roughly unchanged. We find that the bigger nucleon number of the collisions nucleon corresponding to the lower yield ratios of antiparticles to particles. It means that the productions of antimatter in the collisions of light nuclei are easier in the same conditions, and this is suit for the nucleus and particles productions. We can also see that the particles (π^+ , K^+ , p , n , Λ , Ξ^- , and Ω^-) ratios approach to 1, while the hypertriton ($^3_{\Lambda}\text{H}$) and light nuclei (d , t , and ^3He) is less than 1. The results obtained from our models are in agreement with the experimental data from the PHOBOS Collaboration [28].

We show the rapidity distributions of d , t , ^3He , $^3_{\Lambda}\text{H}$ and their antinuclei in $^{12}\text{C}+^{12}\text{C}$, $^{24}\text{Mg}+^{24}\text{Mg}$, $^{40}\text{Ca}+^{40}\text{Ca}$, and $^{64}\text{Cu}+^{64}\text{Cu}$ collisions at $\sqrt{S_{NN}} = 200$ GeV with PACIAE + DCPC models in FIG. 2. The particles and the antiparticles are mainly produced at the mid-rapidity and quickly decrease towards forward (backward) the rapidity. It is obviously that the rapidity distributions of antimatter are less than their corresponding matter with the same nucleus collisions. For the same particles produced, we find that the rapidity distributions raise with the nucleon number of the collision nucleus.

Then we compare the relationship between the nucleon number of the particles produced and their rapidity distributions in the same condition. We find that the rapidity distributions for d are different from those for t , ^3He , and $^3_{\Lambda}\text{H}$, which show the less rapidity distributions than d (a). This is because that d (a) contains two nuclei, while t (b), ^3He (c), and $^3_{\Lambda}\text{H}$ (d) all contain three nuclei. For the same nucleon number nuclei, t (b) and ^3He (c), the former is consists of one proton and two neutron while the latter is consist of two proton and one neutron, we find that the rapidity distributions of t (b) are roughly consistent with the ^3He (c). However, the rapidity value of former is a little bit higher than latter. As shown in FIG. 2, compared with the t (b) (one proton and two neutron) and

TABLE II: The integrated yield dN/dy of particles at midrapidity ($|y| < 0.5$) with 0 – 10% centrality, for d (\bar{d}), t (\bar{t}), ${}^3\text{He}$ ($\overline{{}^3\text{He}}$) and ${}^3_\Lambda\text{H}$ ($\overline{{}^3_\Lambda\text{H}}$) in ${}^{12}\text{C}+{}^{12}\text{C}$, ${}^{24}\text{Mg}+{}^{24}\text{Mg}$, ${}^{40}\text{Ca}+{}^{40}\text{Ca}$, and ${}^{64}\text{Cu}+{}^{64}\text{Cu}$ collisions at $\sqrt{S_{NN}} = 200$ GeV.

Collision types	d	\bar{d}	t	\bar{t}	${}^3\text{He}$	$\overline{{}^3\text{He}}$	${}^3_\Lambda\text{H}$	$\overline{{}^3_\Lambda\text{H}}$
${}^{12}\text{C}+{}^{12}\text{C}$	2.187E-03	1.415E-03	4.227E-07	2.292E-07	3.492E-07	1.721E-07	2.364E-07	1.104E-07
${}^{24}\text{Mg}+{}^{24}\text{Mg}$	7.301E-03	4.598E-03	1.114E-06	5.907E-07	9.121E-07	4.455E-07	6.453E-07	2.942E-07
${}^{40}\text{Ca}+{}^{40}\text{Ca}$	2.094E-02	1.298E-02	2.676E-06	1.391E-06	2.189E-06	1.048E-06	1.722E-06	7.629E-07
${}^{64}\text{Cu}+{}^{64}\text{Cu}$	3.835E-02	2.397E-02	4.181E-06	2.163E-06	3.731E-06	1.780E-06	2.783E-06	1.207E-06

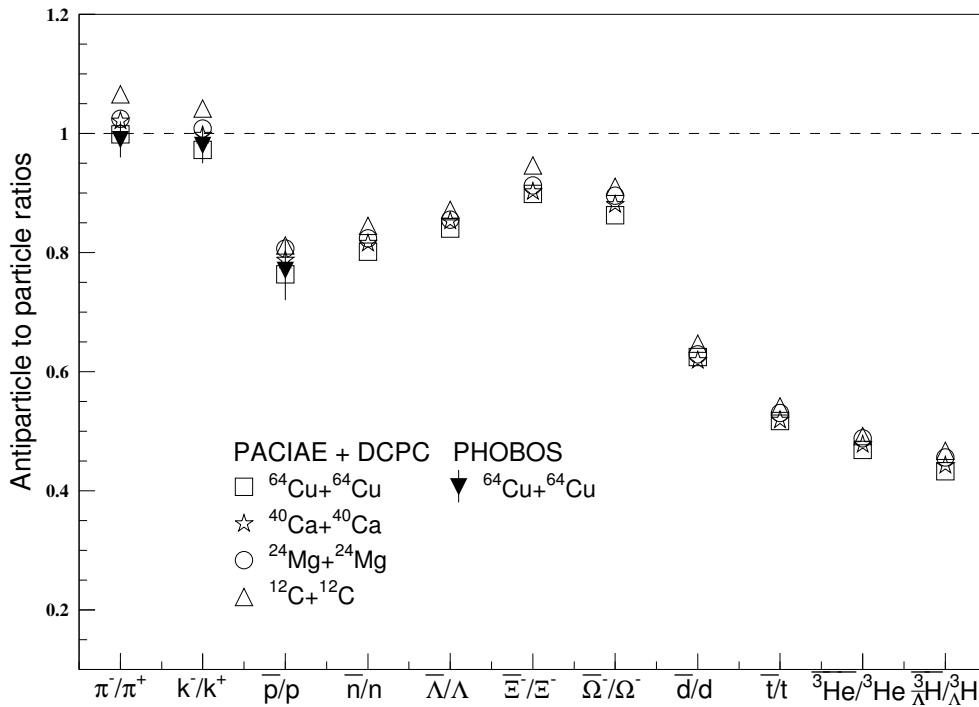


FIG. 1: The yield ratios of particles (π^+ , K^+ , p , n , Λ , Ξ^- , and Ω^-) to corresponding antiparticles (π^- , K^- , \bar{p} , \bar{n} , $\bar{\Lambda}$, $\bar{\Xi}^-$, and $\bar{\Omega}^-$) in 0 – 10% centrality ${}^{12}\text{C}+{}^{12}\text{C}$, ${}^{24}\text{Mg}+{}^{24}\text{Mg}$, ${}^{40}\text{Ca}+{}^{40}\text{Ca}$, and ${}^{64}\text{Cu}+{}^{64}\text{Cu}$ at $\sqrt{S_{NN}} = 200$ GeV reaction. Solid symbols are the experimental data points from the PHOBOS Collaboration [28]. Open symbols represent the PACIAE + DCPC model results.

the ${}^3_\Lambda\text{H}$ (d) (one proton, one neutron, and one Λ), we find that the rapidity distributions of the particles which has (anti-)hyperon is lower than that replaced by a neutron.

The transverse momentum distributions of the ratios for d , t , ${}^3\text{He}$, and ${}^3_\Lambda\text{H}$ to their antiparticles produced in ${}^{12}\text{C}+{}^{12}\text{C}$, ${}^{24}\text{Mg}+{}^{24}\text{Mg}$, ${}^{40}\text{Ca}+{}^{40}\text{Ca}$, and ${}^{64}\text{Cu}+{}^{64}\text{Cu}$ collisions are given in FIG. 3. We find that in the same condition (the nucleon number and the particle production), the ratios of the antiparticle to particle are small at the low transverse momentum regions, while they have a rapidly increase at the high transverse momentum regions. We also find that under the same transverse momentum, the ratios are inversely proportional to the nucleon number of the collision nucleus.

We also compare the relationship between the nucleon number of the particles produced and their antiparticle to particle ratios in the same condition. We find that the ratios of \bar{d}/d (a) is higher than that of \bar{t}/t (b), $\overline{{}^3\text{He}}/{}^3\text{He}$ (c), and $\overline{{}^3_\Lambda\text{H}}/{}^3_\Lambda\text{H}$ (d), because of the two nuclei d , and the others are three. For the same nucleon number nuclei, the antiparticle to particle ratios of \bar{t}/t (b), $\overline{{}^3\text{He}}/{}^3\text{He}$ (c), and $\overline{{}^3_\Lambda\text{H}}/{}^3_\Lambda\text{H}$ (d) have a similar distributions.

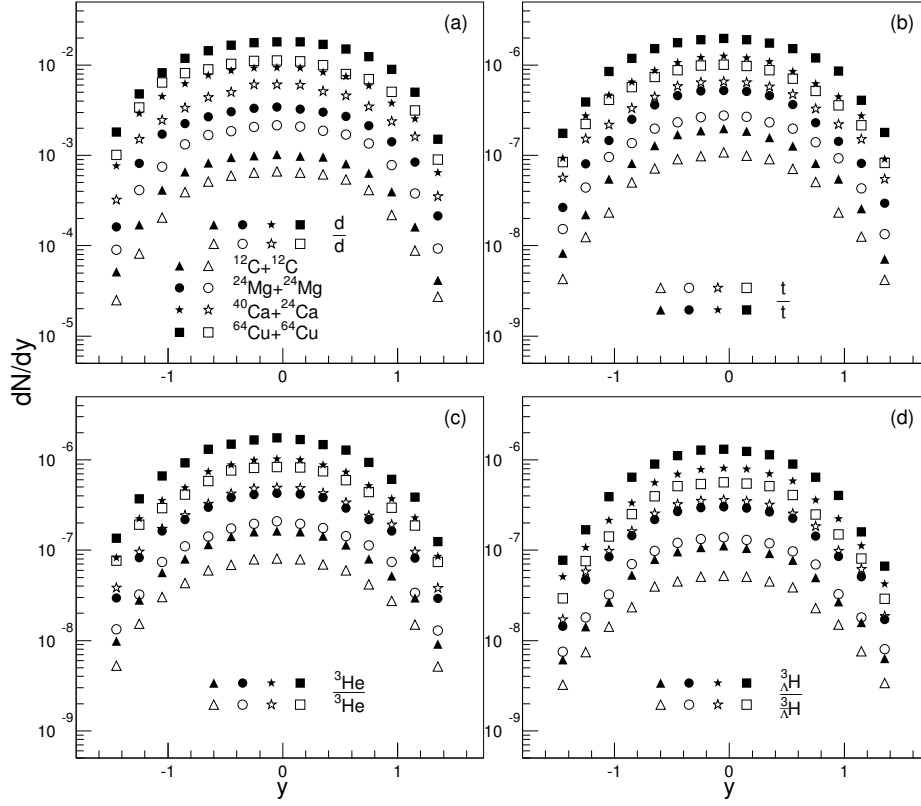


FIG. 2: The rapidity ($|y| < 1.5$) distributions of particles d (a), t (b), ${}^3\text{He}$ (c), and ${}^3_{\Lambda}\text{H}$ (d) to corresponding antiparticles \bar{d} (a), \bar{t} (b), $\bar{{}^3\text{He}}$ (c), and $\bar{{}^3_{\Lambda}\text{H}}$ (d) produced by PACIAE + DCPC model at $\sqrt{S_{NN}} = 200$ GeV in 0 – 10% centrality ${}^{12}\text{C}+{}^{12}\text{C}$, ${}^{24}\text{Mg}+{}^{24}\text{Mg}$, ${}^{40}\text{Ca}+{}^{40}\text{Ca}$, and ${}^{64}\text{Cu}+{}^{64}\text{Cu}$ collisions.

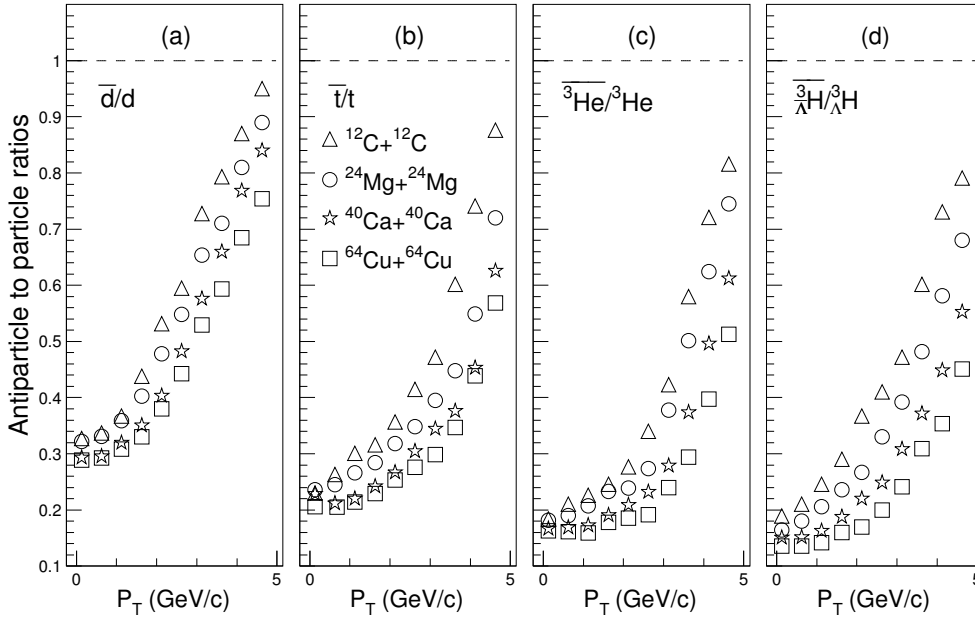


FIG. 3: The p_T dependence of the ratios for antiparticles (\bar{d} , \bar{t} , $\bar{{}^3\text{He}}$, and $\bar{{}^3_{\Lambda}\text{H}}$) to particles (d , t , ${}^3\text{He}$, and ${}^3_{\Lambda}\text{H}$) produced by PACIAE + DCPC model at $\sqrt{S_{NN}} = 200$ GeV in 0 – 10% centrality ${}^{12}\text{C}+{}^{12}\text{C}$, ${}^{24}\text{Mg}+{}^{24}\text{Mg}$, ${}^{40}\text{Ca}+{}^{40}\text{Ca}$, and ${}^{64}\text{Cu}+{}^{64}\text{Cu}$ collisions. The transverse momentum range is 0 – 5 GeV/c.

IV. CONCLUSION

In this work, we use the PACIAE + DCPC models to investigate the productions of (anti)hypertriton and light (anti)nuclei generated by 0 – 10% central $^{12}\text{C}+^{12}\text{C}$, $^{24}\text{Mg}+^{24}\text{Mg}$, $^{40}\text{Ca}+^{40}\text{Ca}$, and $^{64}\text{Cu}+^{64}\text{Cu}$ collisions at $\sqrt{S_{NN}} = 200$ GeV with $|y| < 1.5$ and $p_T < 5$. We study the yield ratios of antiparticle to particle and the rapidity distributions of the different (anti)nuclei. The results obtained from our models are in agreement with the experimental data from the PHOBOS Collaboration. It is obviously that the rapidity distributions of antimatter are less than their corresponding matter with the same nucleus collisions. The yield ratios of the particles in different transverse momentum regions are also given. We find that the ratios are raise with the increase of the transverse momentum, the ratios of the antiparticle to particle are small at the low transverse momentum regions while they have a rapidly increase at the high transverse momentum regions.

ACKNOWLEDGMENT

This work is supported by the NSFC (Grants No. 11305144 and No. 11303023) and SPIE (Grant No. 201310491051) in China.

-
- [1] P. A. M. Dirac, Proc. Roy. Soc. Lond. A **117**, 610 (1928).
 - [2] G. Gamow, Phys. Rev. **70**, 572 (1946).
 - [3] P. von Ballmoos, Hyperfine Interact. **228**, 91 (2014), 1401.7258.
 - [4] J.-L. Wang, G. Chen, H.-J. Li, and D.-K. Li, Int. J. Mod. Phys. E **23**, 1450088 (2014), 1409.7884.
 - [5] G. Chen, Y.-L. Yan, D.-S. Li, D.-M. Zhou, M.-J. Wang, B.-G. Dong, and B.-H. Sa, Phys. Rev. C **86**, 054910 (2012), 1209.4182.
 - [6] S. Ahlen et al., Nucl. Instrum. Meth. A **350**, 351 (1994).
 - [7] M. Casolino et al., Adv. Space Res. **42**, 455 (2008), 0708.1808.
 - [8] D. Dorfan, J. Eades, L. Lederman, W. Lee, C. Ting, P. Piroue, S. Smith, J. Brown, J. Kadyk, and G. Trilling, Phys. Rev. Lett. **14**, 995 (1965).
 - [9] S. Adler et al. (PHENIX), Phys. Rev. Lett. **94**, 122302 (2005), nucl-ex/0406004.
 - [10] Y.-G. Ma, J.-H. Chen, and L. Xue, Front. Phys. (Beijing) **7**, 637 (2012), 1301.4902.
 - [11] L. Bergstrom, AIP Conf. Proc. **478**, 352 (1999), astro-ph/9902172.
 - [12] S. Zhang, J.-H. Chen, Y.-G. Ma, Z.-B. Xu, X.-Z. Cai, G.-L. Ma, and C. Zhong, Chin. Phys. C **35**, 741 (2011).
 - [13] J. Schaffner and I. N. Mishustin, Phys. Rev. C **53**, 1416 (1996), nucl-th/9506011.
 - [14] F. Hofmann, C. Keil, and H. Lenske, Phys. Rev. C **64**, 025804 (2001), nucl-th/0008038.
 - [15] B. Abelev et al. (STAR), Science **328**, 58 (2010), 1003.2030.
 - [16] H. Agakishiev et al. (STAR), Nature **473**, 353 (2011), [Erratum: Nature 475, 412 (2011)], 1103.3312.
 - [17] Y.-L. Yan, G. Chen, X.-M. Li, D.-M. Zhou, M.-J. Wang, S.-Y. Hu, L. Ye, and B.-H. Sa, Phys. Rev. C **85**, 024907 (2012), 1107.3207.
 - [18] Y.-L. Yan, D.-M. Zhou, B.-G. Dong, X.-M. Li, H.-L. Ma, and B.-H. Sa, Phys. Rev. C **81**, 044914 (2010), 1001.1595.
 - [19] B.-H. Sa, D.-M. Zhou, Y.-L. Yan, B.-G. Dong, and X. Cai, Comput. Phys. Commun. **184**, 1476 (2013), 1206.4795.
 - [20] G. Chen, H. Chen, J. Wu, D.-S. Li, and M.-J. Wang, Phys. Rev. C **88**, 034908 (2013), 1307.4515.
 - [21] G. Chen, H. Chen, J.-L. Wang, and Z.-Y. Chen, J. Phys. G **41**, 115102 (2014), 1401.6872.
 - [22] T. Sjostrand, S. Mrenna, and P. Z. Skands, JHEP **05**, 026 (2006), hep-ph/0603175.
 - [23] B. Combridge, J. Kripfganz, and J. Ranft, Phys. Lett. B **70**, 234 (1977).
 - [24] B. Sa and A. Tai, Comput. Phys. Commun. **90**, 121 (1995).
 - [25] A. Tai and B.-H. Sa, Comput. Phys. Commun. **116**, 353 (1999), nucl-th/9804001.
 - [26] T. Chujo (PHENIX), Eur. Phys. J. C **49**, 23 (2007), nucl-ex/0608020.
 - [27] G. Agakishiev et al. (STAR), Phys. Rev. Lett. **108**, 072301 (2012), 1107.2955.
 - [28] B. Alver et al. (PHOBOS), Phys. Rev. C **77**, 061901 (2008), 0802.1695.